

Supplementary material to: Modelling debris transport within glaciers by advection in a full-Stokes ice flow model.

Anna Wirbel¹, Alexander H. Jarosch², and Lindsey Nicholson¹

¹Institute of Atmospheric and Cryospheric Sciences, University of Innsbruck, Innsbruck, Austria

²Institute of Earth Sciences, University of Iceland, Reykjavík, Iceland.

Appendix A: Benchmark tests

A1 Numerical tests following Bochev et al. (2004)

We reproduce the Numerical Examples in Bochev et al. (2004). Initial and boundary conditions are initialized in the same manner as described for Example 1 and 2 in Bochev et al. (2004). The computations are performed on an unstructured mesh built out of 874 triangular elements, created with *gmsh* (Geuzaine and Remacle, 2009). The concentration is set up in a continuous piecewise linear function space, resulting in 1821 degrees of freedom. In Fig. A1a, the cell size parameter used for the SUPG (Streamline-Upwind-Petrov-Galerkin) - stabilisation term is shown in colour with the underlying unstructured mesh. In Figs. A1(b-c) the velocity fields of Example 1 and 2 are illustrated.

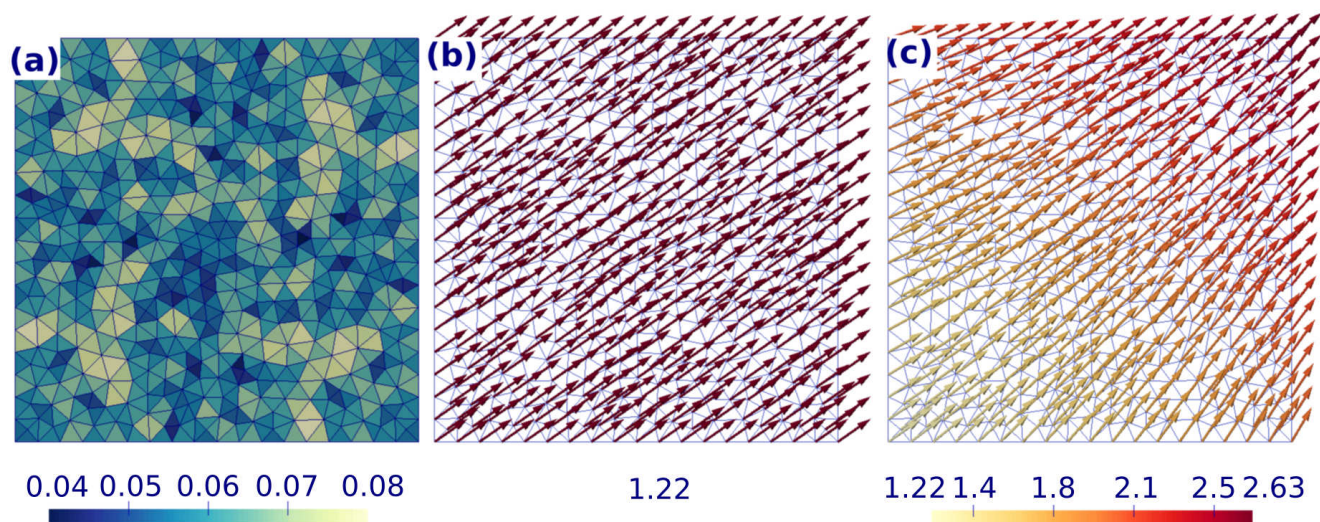


Figure A1. In (a) the mesh cell size parameter, in (b) and (c) the velocity fields for Examples 1 and 2 are shown.

Following Bochev et al. (2004), the computations are performed for four different time steps: $dt = 0.1$, $dt = 0.01$, $dt = 0.001$, $dt = 0.0005$. In Fig. A2, results of Example 1 at total time $t = 0.5$, cross-profiles at $y = 0.6$ and at $x = 0.75$, for all four time step settings respectively, are shown. In Fig. A3, results of Example 2 at total time $t = 0.5$, cross-profile at $y = 0.85$ and at $x = 1.0$, for all four time step settings respectively, are shown. The results of Example 1 and 2 are in good agreement with the published results in Bochev et al. (2004). The oscillations are stronger, which is mainly caused by the stronger irregularity in mesh cell size in our tests.

Table 1. This table lists the H1 semi-norm for different time steps and Courant-Friedrich-Levy condition parameters, for examples 1 and 2.

Δt	0.1	0.01	0.001	0.0005
example 1				
$CFL - constant_{mean}$	2.7671	0.2767	0.02767	0.01383
H1 semi-norm	7.3429	4.7117	4.6537	4.65319
example 2				
$CFL - constant_{max}$	4.88407	0.488407	0.0488407	0.0244203
H1 semi-norm	7.5497	3.3116	3.26708	3.26658

A2 Numerical tests following de Frutos et al. (2014)

In this Section, additional figures presenting the results of the "rotating three body problem" (de Frutos et al., 2014) are shown. The initial condition, the solution after one full rotation and the over- and undershoots in the solution after one full rotation are illustrated in Fig. A4. In comparison to the refinement time step of 0.1π presented in the paper, we here employ a refinement time step of 0.01π . The results demonstrate that the choice of the refinement time step does not affect the quality of the results. Additionally, we reproduced the three body test with swirling flow conditions (LeVeque, 1996). In Fig. A5 the results of simulations using a refinement time step of 0.1π , compared to the refinement time step of 0.01π used in the paper, are shown.

15 A3 ISMIP Benchmark test

In order to be able to compare the ice velocities of Haute Glacier d'Arolla computed with *icetools*, to the results of the Ice Sheet Model Intercomparison Project in Pattyn et al. (2008), the computations have been performed using $A = 10^{-16} \text{ a}^{-1} \text{ Pa}^{-3}$. The simulated surface velocity is shown in Fig. A6.

References

- Bochev, P. B., Gunzburger, M. D., and Shadid, J. N.: Stability of the SUPG finite element method for transient advection–diffusion problems, *Comput. Method. Appl. M.*, 193, 2301–2323, doi:10.1016/j.cma.2004.01.026, 2004.
- de Frutos, J., García-Archilla, B., John, V., and Novo, J.: An adaptive SUPG method for evolutionary convection–diffusion equations, *Comput. Method. Appl. M.*, 273, 219–237, doi:10.1016/j.cma.2014.01.022, 2014.
- 5 Geuzaine, C. and Remacle, J.-F.: Gmsh: A 3-D finite element mesh generator with built-in pre-and post-processing facilities, *Int. J. Numer. Meth. Eng.*, 79, 1309–1331, 2009.
- LeVeque, R.: High-Resolution Conservative Algorithms for Advection in Incompressible Flow, *SIAM J. Numer. A.*, 33, 627–665, doi:10.1137/0733033, 1996.
- 10 Pattyn, F., Perichon, L., Aschwanden, A., Breuer, B., de Smedt, B., Gagliardini, O., Gudmundsson, G. H., Hindmarsh, R. C. A., Hubbard, A., Johnson, J. V., Kleiner, T., Konovalov, Y., Martin, C., Payne, A. J., Pollard, D., Price, S., Rückamp, M., Saito, F., Souček, O., Sugiyama, S., and Zwinger, T.: Benchmark experiments for higher-order and full-Stokes ice sheet models (ISMIP–HOM), *The Cryosphere*, 2, 95–108, doi:10.5194/tc-2-95-2008, 2008.

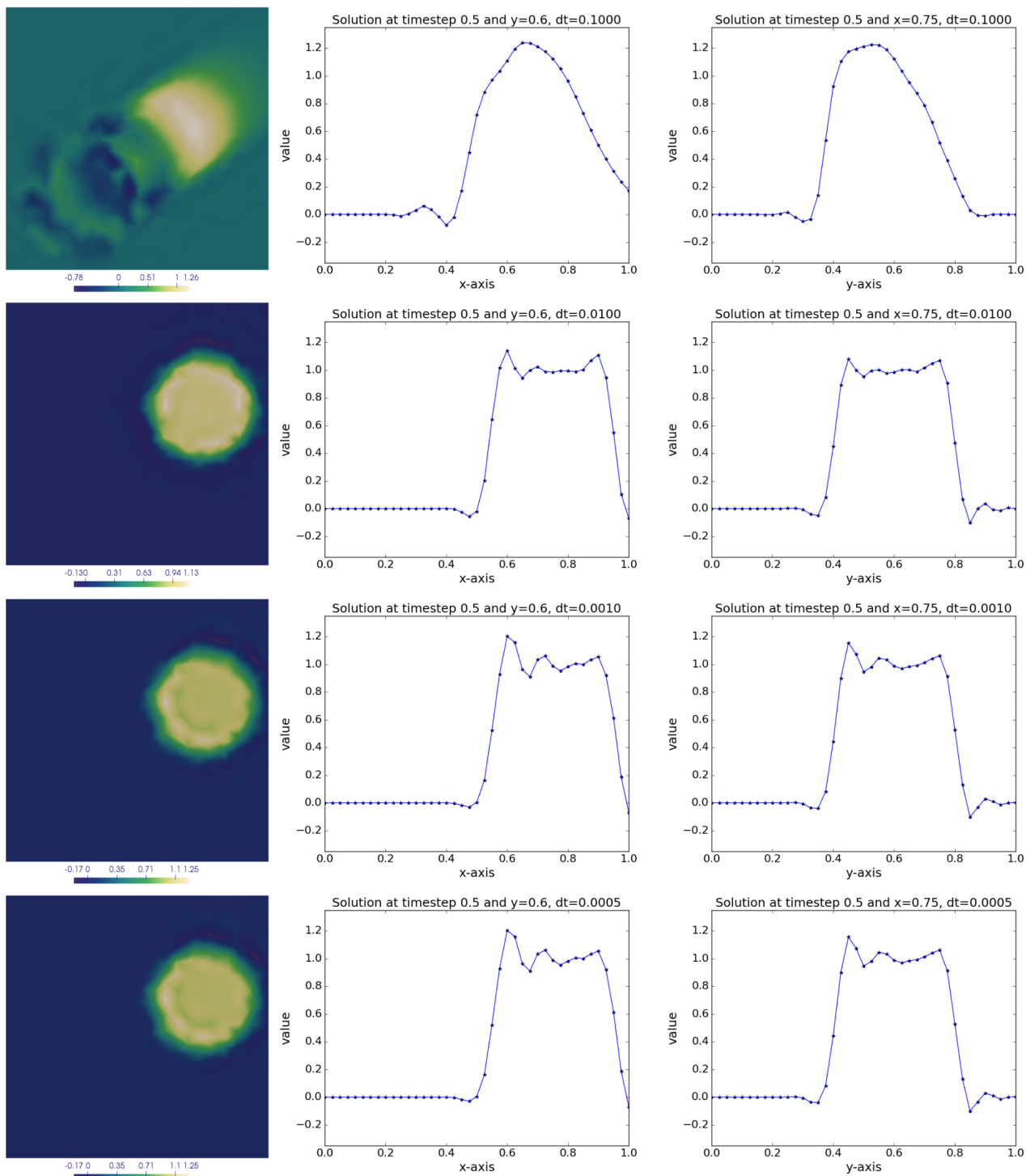


Figure A2. Results of Numerical Example 1. Solutions at $t = 0.5$, cross-profiles at $y = 0.6$ and cross-profiles at $x = 0.75$ for (top to bottom): $dt = 0.1$, $dt = 0.01$, $dt = 0.001$, $dt = 0.0005$.

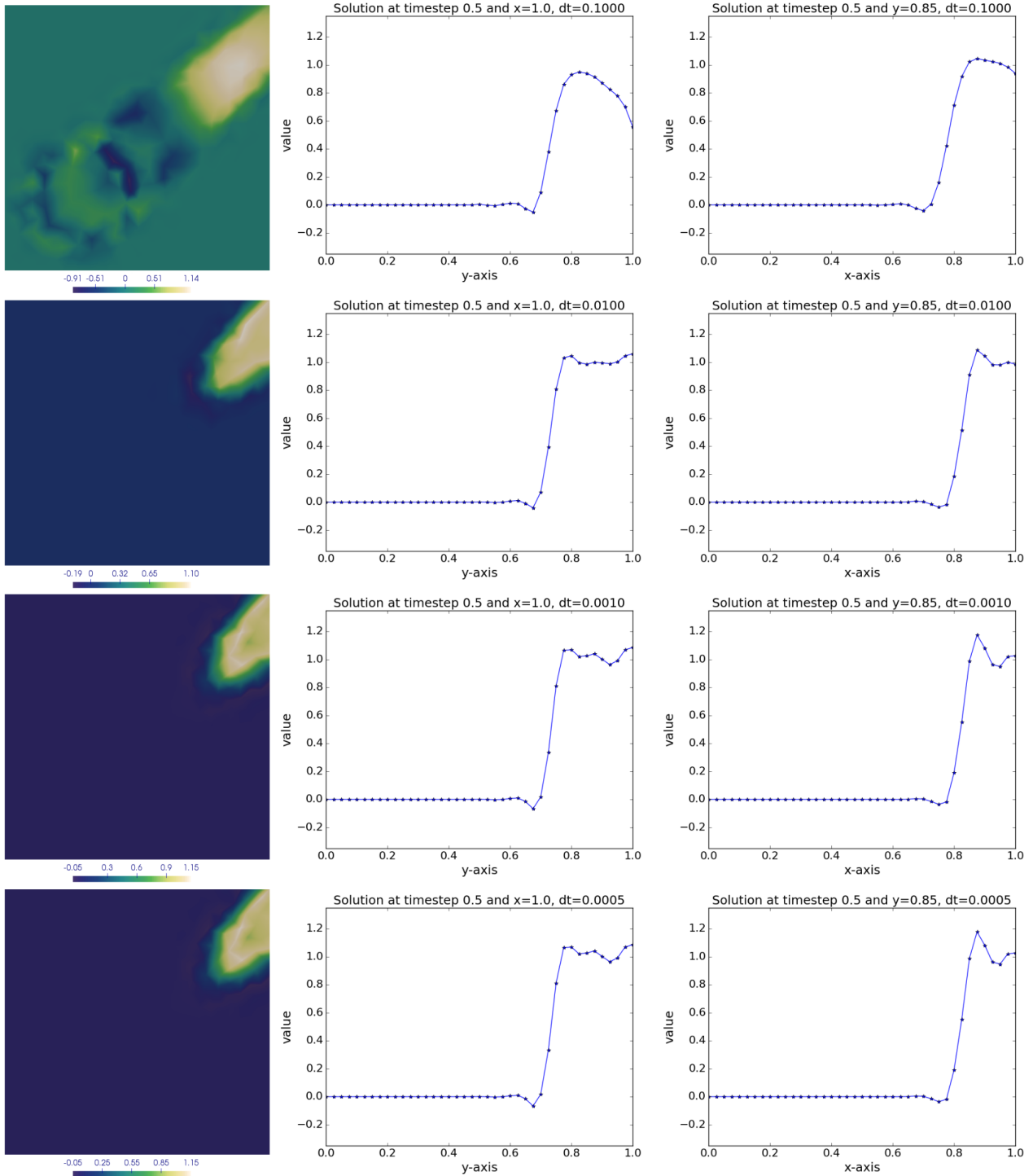


Figure A3. Results of Numerical Example 2. Solutions at $t = 0.5$, cross-profiles at $y = 0.85$ and cross-profiles at $x = 1.0$ for (top to bottom): $dt = 0.1$, $dt = 0.01$, $dt = 0.0001$, $dt = 0.00005$.

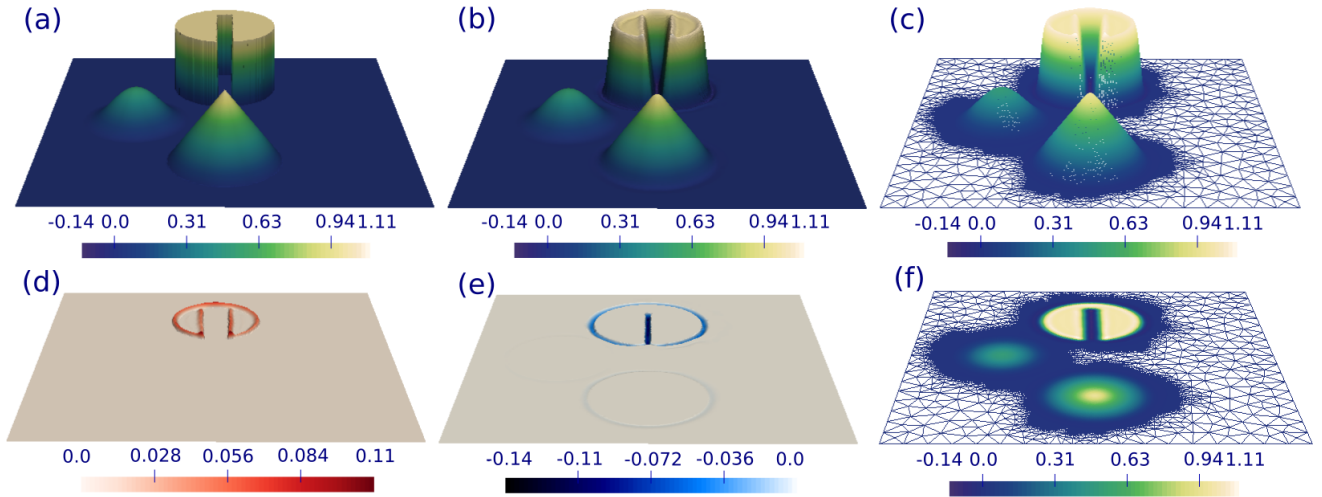


Figure A4. Results of 2D three body rotation test for refinement time step 0.01π . In (a) the initial condition, in (b) the solution after one full rotation and in (c) the solution after one full rotation on the underlying mesh is shown. The data ranges from -0.14 to 1.11 . In (d) overshoots (values greater than maximum initial value, as deviation from $\max(c_{initial}) = 1.0$) and in (e) undershoots (values smaller than minimum initial value, as deviation from $\min(c_{initial}) = 0.0$) at T are presented. In (f) the solution after one full rotation on the underlying mesh is shown in plan view. Colourscales show concentration values.

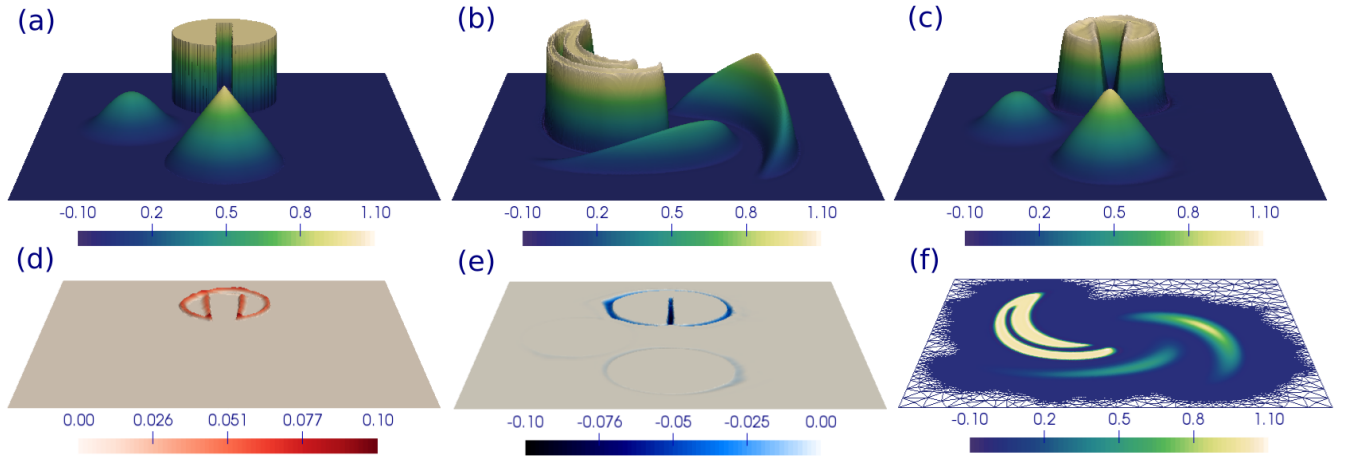


Figure A5. Results of 2D swirling flow three body test for refinement time step 0.1π . In (a) the initial condition, in (b) the solution at $T/2$ and in (c) the solution at total time T is shown. The data ranges from -0.1 to 1.1 . In (d) overshoots (values greater than maximum initial value, as deviation from $\max(c_{initial}) = 1.0$) and in (e) undershoots (values smaller than minimum initial value, as deviation from $\min(c_{initial}) = 0.0$) at T are presented. In (f) the solution at $T/2$ on the underlying mesh is shown in plan view. Colourscales show concentration values.

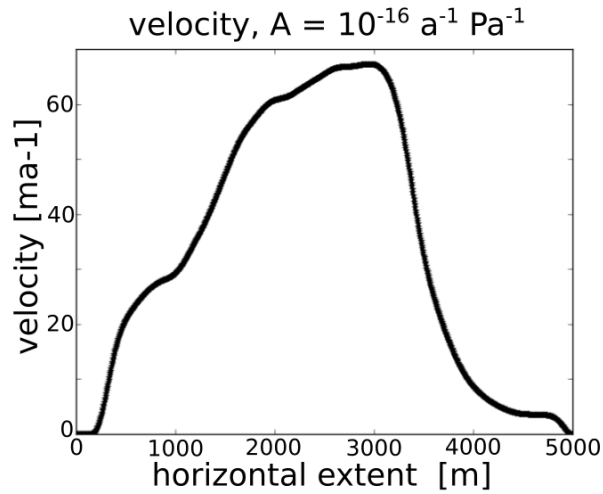


Figure A6. Surface velocity (ma^{-1}) of the longprofile of Haut Glacier d'Arolla computed with $A = 10^{-16} \text{ a}^{-1} \text{ Pa}^{-3}$.